Stereoelectronic Interactions and Molecular Properties. An NBO-Based Study of Uracil

Eduardo M. Sproviero and Gerardo Burton*

Departamento de Química Orgánica, Facultad de Ciencias Exactas y Naturales, Universidad de Buenos Aires, Pabellón 2, Ciudad Universitaria, (C1428EGA) Buenos Aires, Argentina

Received: October 10, 2002; In Final Form: May 9, 2003

The contributions of stereoelectronic interactions to several molecular properties are used to analyze the propagation of information between different parts of the uracil molecule with a method that is based on the natural bond orbital (NBO) deletion technique. The emphasis is not on the effect of the contributions of localized orbitals to selected properties but rather on their interactions, giving information that is complementary to that resulting from a standard localized molecular orbital contribution. The analysis of how information between orbitals is transmitted throughout the molecule allows interpretation of the ways in which an interaction can affect a molecular property localized in the same region or in a different region of the molecule. A network of stereoelectronic interactions was identified in the uracil molecule, and the relative influences of the interactions that transmit information between different parts of the molecule were evaluated. An analysis was performed over localized properties on atoms and bonds of the two carbonyl groups, namely bond orders, distribution of electronic charge, and NMR shielding tensors. Interactions $n(N_3) \rightarrow \pi^*(C_4{=}O)$ and $n(N_1) \rightarrow \pi^*(C_5{=}C_6)$ were the most important delocalizations that carry information concerning the change of substituents at C-5, whereas interactions $n(N_1) \rightarrow \pi^*(C_2{=}O)$ and $n(N_3) \rightarrow \pi^*(C_2{=}O)$ were those mainly responsible for transmitting this information to the C-2 uracil carbonyl ($C_2{=}O$) properties.

1. Introduction

In the very basis of chemical thought lies the image of molecules as being composed of atoms, linked with bonds, with localized electrons in nonbonding lone pairs. This picture depicts that of a Lewis-type molecule.[1] Indeed, this is the underlying idea in most chemical models, which offer a vivid description of the electronic density of molecules that is useful in many chemical problems. It is noteworthy that even the simplest models give a pictorial representation of the charge distribution that may be used to analyze chemical effects, rationalize chemical reactivity, or search for empirical correlations among different types of experimental results. From a theoretical point of view, several methods give a set of localized molecular orbitals (LMOs) that are equivalent to the delocalized canonical set of molecular orbitals, such as the Foster−Boys,[2] Edmiston−Ruedenberg,[3] Weinstein et al.,[4] or Weinhold's natural bond orbital (NBO)[5−8] approaches. Strictly speaking, these "chemical thought" orbitals suffer small departures from the idealized Lewis structure, caused by interactions among them, known as hyperconjugative or stereoelectronic interactions.[9] These interactions connect a donor-type orbital with an acceptor-type orbital, implying a net transfer of charge. The new orbitals are more stable than pure Lewis orbitals, stabilizing the wave function and giving a set of molecular orbitals equivalent to canonical molecular orbitals.

Several methods have been used to analyze the contribution of localized orbitals to molecular properties.[10−20] Only recently have methods that emphasize the evaluation of the delocalization contributions been developed,[19,21,22] although an estimation of these contributions to specific properties has also been made indirectly, within the framework of bond localization formalisms.[23−26]

In addition to the stabilization feature, the stereoelectronic interactions also provide a way to transmit information between different parts of the molecule. For example, NBO-based methods have been used to establish through-bond coupling or, equivalently, superexchange in electron-transfer reactions of donor−bridge−acceptor compounds.[27−29] Recently, we analyzed the effect of hyperconjugative interactions by a combination of NBO deletion techniques and electron polarization propagator methods for evaluating delocalization contributions to scalar J-coupling.[21] A natural extension of this methodology leads to a generalization of the combination of the NBO deletion procedure with the calculation of any molecular property.

In this work, we present a method based on the NBO[5−8] approach for the evaluation of the contribution of delocalization interactions to molecular properties. Any property that is dependent on a polyatomic wave function describing the molecular system (e.g., electronic charge density, atomic charges, bond orders, or shielding tensors) is susceptible of being analyzed, allowing a numerical estimation of the contribution of stereoelectronic interactions to selected molecular properties. Furthermore, as the procedure involves the deletion of selected elements of a one-electron effective Hamiltonian operator it is applicable whenever such types of operators are well defined, e.g., Fock or Kohn−Sham operators, involved in ab initio/semiempirical wave functions or density functional theory (DFT) states.

At variance with other methods that analyze delocalization contributions,[19,22] the present formalism does not require special programming, but rather needs a suitable combination of the NBO deletion method with the calculation of properties within a single electronic structure package or a combination of different packages. This makes the method easily applicable to any property that can be calculated from the many-electron molecular wave function. An additional difference from other methods is that the emphasis is not on the effect of the

* Author to whom correspondence should be addressed. E-mail: burton@qo.fcen.uba.ar.

10.1021/jp0271763 CCC: $25.00
Published on Web 06/26/2003

SCHEME 1: Flow Chart of the Implementation of the NBO-Based Deletion Method

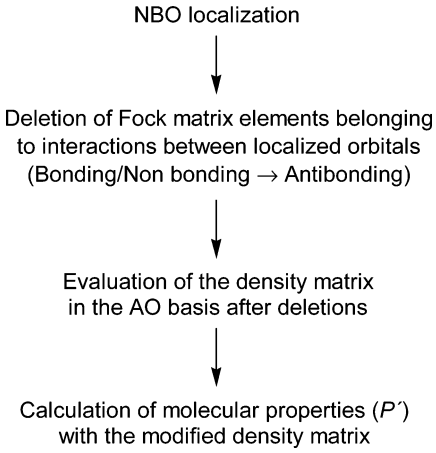

contributions of localized orbitals to selected properties[10−20] but rather on their interactions, giving information that is complementary to that resulting from a standard LMO contribution. The analysis of how information between orbitals is transmitted throughout the molecule allows interpretion of the ways in which an interaction can affect a molecular property localized in the same region or in a different region of the molecule. In this respect, the superexchange model used to analyze electron transfer includes all pathways through the bonding and antibonding manifolds of orbitals, except those which cross between the two manifolds. Our approach differs from the superexchange one, because the absence of high-energy intermediate states leads to donor → acceptor orbital delocalizations as building blocks of the pathway of transmission of information.

The methodology presented in this work is used to analyze the contributions of stereoelectronic interactions to bond orders, electronic charges, and nuclear magnetic shielding tensors that are associated with carbonyl groups in uracil and 5-substituted uracils.

2. Methods

Geometry optimizations, bond orders, atomic charges, nuclear shielding calculations, and natural bond orbital (NBO) analysis were conducted using the Gaussian 98 suite of programs.[30] NBO analysis was used to evaluate delocalization effects using the RESONANCE keyword, which permits a strongly delocalized structure. These calculations were performed with module 3.11[31] of the Gaussian 98 package of programs. Optimized geometries were computed at the RHF/6-31G** level of theory. Single-point calculations, including NBO analysis, were done at the RHF/6-31+G** level of theory; charge density calculations were performed at the 6-311+G(2d,p) level. Furthermore, because the relative intensities of NBO deletion energies are not very sensitive to improvements in the basis set, the same RHF/6-31+G** basis set was chosen for the deletion-based analysis.

A computational procedure was used in this study. The methodology, which is based on NBO deletions,[21] is briefly described in Scheme 1 and was implemented by means of a combination of several modules of the Gaussian 98 program, using a nonstandard route. After definition of a usual route including basis set information, symmetry of the wave function, and a SCF calculation, an NBO localization is made, followed by a standard deletion procedure. Then, one step of a SCF optimization is made to relax the resulting wave function and keep the molecular system from being too far from a variational minimum. The entire procedure is recorded in a Gaussian scratch file, such that the molecular orbital coefficients correspond to the wave function with the deleted interactions. Afterward, a series of modules of the Gaussian 98 package are used to calculate selected response properties, following the conventional procedure for each module (see the electronic Supporting Information for full details and a specific example).

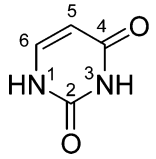

Figure 1. Uracil molecule with the usual atomic numbering.

The magnitudes calculated with the method previously described were compared with those obtained without deletions, thus allowing evaluation of the relative contributions of the interactions involved. If P is the value of a molecular property obtained with the complete Fock matrix and P' is the calculated value with the deletion of selected interactions, then the difference $\Delta P \equiv P - P'$ may be considered to be proportional to the contribution of the corresponding interactions to the property under study and may thus be used to evaluate the relative contributions of different interactions to the selected property.

3. Results and Discussion

Uracil (Figure 1) was selected as a model compound to test the present formalism, taking into account, besides the high biological relevance, its structural features. As expected from the study of coupling constants[21] and the magnitudes of the corresponding delocalization energies, vicinal interactions are the best candidates to influence molecular properties and to transmit information within the molecular framework; uracil presents all types of vicinal interactions ($\sigma \rightarrow \sigma^*$, $\sigma \rightarrow \pi^*$, $\pi \rightarrow \sigma^*$, $\pi \rightarrow \pi^*$, $n \rightarrow \sigma^*$, and $n \rightarrow \pi^*$), which result in a high degree of delocalization. In comparison to a linear molecule, a cyclic compound such as this provides a more versatile frame with several transmission paths.[26] We focused our attention on the analysis of how stereoelectronic interactions affect the properties of the carbonyl oxygen atoms, considering their importance in the hydrogen bonding interactions that are present when uracil forms part of the RNA molecule.

We were interested in understanding the role that electronic delocalizations play over two groups of molecular properties: those derived from the distribution of charge and those derived from the distribution of current. Although the former may be evaluated directly from the ground-state wave function, the electronic current is a response of the system to the application of external electromagnetic fields; therefore, it cannot be calculated from the unperturbed ground-state wave function alone. Thus, properties associated with the electronic current must be calculated from the first-order correction that results from the application of an external field, according to the usual procedure of perturbation theory. Interactions between orbitals affect both types of properties in different ways. In the case of charge distribution, a direct effect on the charge density results from alteration of the contributing orbitals. In the case of applying a magnetic field, an indirect effect results from the perturbation via occupied−vacant excitations.

Within the present formalism, it is possible to evaluate all types of electronically derived properties; thus, even the stereoelectronic interactions themselves are suitable to be analyzed. Therefore, a network of interactions results, shedding

light on the mechanisms by which information is propagated within the molecule through delocalization interactions. In this way, the present methodology is consistent with the electronic mechanism by which a polar substituent conveys its influence to a remote probe (energy- or charge-density monitor) in saturated organic systems, by way of the so-called σ-inductive or hyperconjugative effect.[9] This behavior is a consequence of the fact that the NBO localization procedure is a donor−acceptor methodology or a "chemical" approach, in some sense opposite to a fieldlike or "physical" point of view, as discussed by Reed et al.[32] In the same line, NBO concepts have been used to qualitatively rationalize enthalpic factors that stabilize certain H-bond clusters over others. This analysis shows that cluster stability is strongly enhanced if each H-bond is directed to give maximally concerted (cooperative) charge-transfer patterns.[33]

Several properties that are associated with the charge density (being physical observables or not) may be calculated over a given individual atom. In a molecular system, the replacement of a substituent, a conformational change, or the application of an external disturbance results in a variation of the charge density, which results in a concomitant change of the property value. This may be subsequently analyzed in terms of the propagation of information mediated by delocalization interactions.

We first present an analysis of stereoelectronic interactions, which shows their relative importance, their interrelations, and their effect on the electronic density. Then, a systematic study of selected properties is presented that include carbonyl bond orders, atomic population analysis, and ^{17}O magnetic nuclear shieldings.

3.1. Stereoelectronic Interactions. Stereoelectronic interactions between a bonding or nonbonding orbital *i* and an antibonding orbital *j** cause an energy lowering, relative to the idealized Lewis-type structure. Within the NBO perturbative framework, qualitative concepts such as the relation between the strengths of the perturbative Fock matrix elements and the shapes of the NBO bond and antibond orbitals may be applied, allowing the energy lowerings to be described in terms of a principle of maximum overlap. This lowering is well approximated by perturbative expressions as the so-called "second order energy lowering", $E^{(2)}_{ij*}$:[32]

$$E^{(2)}_{ij*} = -2\left(\frac{S^2_{ij*}}{E_{j*} - E_i}\right) \qquad (1)$$

where S_{ij} is the element of the Fock matrix and E_i and E_{j*} are the corresponding orbital energies.

To simplify notation, numbers were assigned to the most relevant stereoelectronic interactions, as shown in Figure 2. Interactions *1* and *2*, which involve the C_4═O carbonyl, may be considered "equivalent" to interactions *3* and *4*, which include the equivalent antibond that involves the C_2═O carbonyl. Similarly, interactions *6* and *7*, which involve the π-type lone pair nonbonding orbital of O_4, are equivalent to interactions *8* and *9*, which involve the π-type lone pair of O_2. As shown below, most of the properties are affected in a similar manner by equivalent interactions.

A direct connection exists between NBO delocalizations and resonance structures.[34] As shown in Figure 2, interactions *1*−*9* can be expressed, in the language of resonance theory, as a correction due to an additional resonance substructure. Thus, when considering the effect of an interaction, the distribution of charge due to a particular resonance substructure is highlighted. Although there is no fundamental distinction between resonance and delocalization (insofar as both terms express departures from a single idealized Lewis structure), these resonance mappings are useful to interpret changes in molecular properties, especially those related to the electronic charge density.

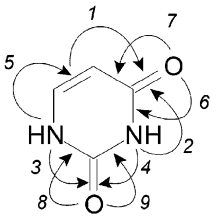

Interaction	Orbitals involved	Resonance substructures
1	$\pi(C_5{=}C_6) \rightarrow \pi^*(C_4{=}O)$	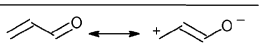
2	$n(N_3) \rightarrow \pi^*(C_4{=}O)$	
3	$n(N_1) \rightarrow \pi^*(C_2{=}O)$	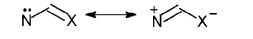
4	$n(N_3) \rightarrow \pi^*(C_2{=}O)$	X = C,O
5	$n(N_1) \rightarrow \pi^*(C_5{=}C_6)$	
6	$n_\pi(O_4) \rightarrow \sigma^*(C_4{-}N_3)$	
7	$n_\pi(O_4) \rightarrow \sigma^*(C_4{-}C_5)$	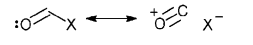
8	$n_\pi(O_2) \rightarrow \sigma^*(C_2{-}N_1)$	X = C,N
9	$n_\pi(O_2) \rightarrow \sigma^*(C_2{-}N_3)$	

Figure 2. Main stereoelectronic interactions present in the uracil molecule, and their equivalent resonance substructures.

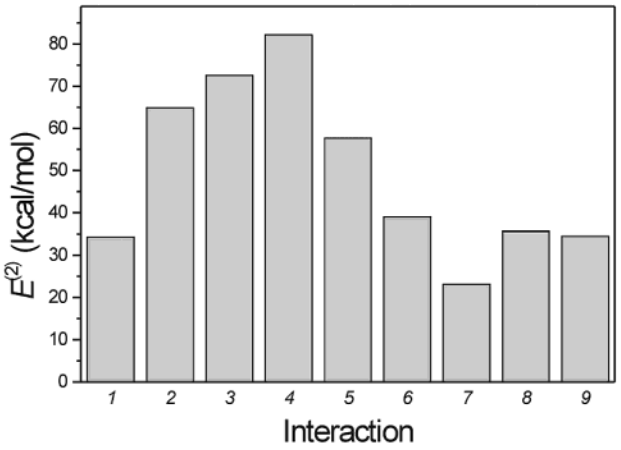

Figure 3. Second-order energy lowering ($E^{(2)}_{ij*}$) values for the main stereoelectronic interactions in uracil (see Figure 2 for notation).

As expected from their equivalent resonance substructures, interactions of the type n(N) → π^*(C═O)/π^*(C═C) (interactions *2*−*5*) have larger $E^{(2)}$ values than those of the form n_π(O) → σ^*(C−C/N) (interactions *6*−*9*) (Figure 3). Interaction *1*, which also involves the antibonding π^*(C═O) orbital, is less intense than interactions *2*−*5*; in this case, energies of the σ-(C═C) and n(N) orbitals are almost equal (−0.41 au, and −0.42 to −0.41 au, respectively), but the Fock matrix element of interaction *1* ($S_{\pi(C=C),\pi^*(C_4=O)} = 0.132$ au) is smaller than the corresponding element that involves a lone-pair donor orbital (e.g., $S_{n(N_3),\pi^*(C_4=O)} = 0.180$ au). The difference in relative intensities of interactions *6* and *7* is a consequence of the different types of atoms that are involved in the acceptor orbitals; in the corresponding resonant substructures, this is evident from the $N^{(-)}$ species being more stable than the $C^{(-)}$ species. Other intensity differences of the interactions within each group result mainly from mutual influences between interactions, which is a topic that will be discussed in detail in the next section.

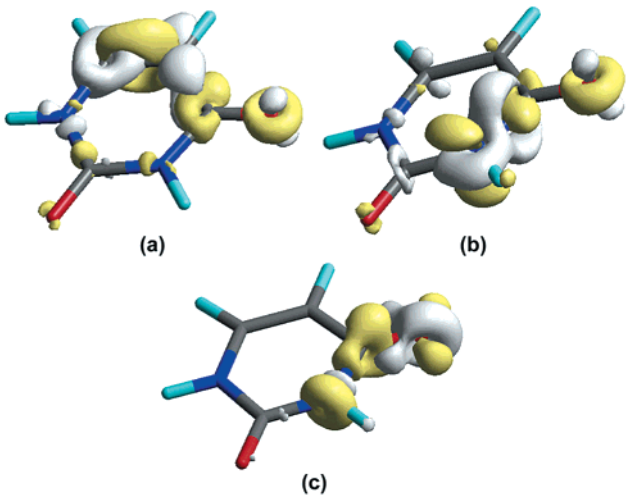

Figure 4. Isodensity diagrams showing the response of the electronic charge density to the deletion of selected stereoelectronic interactions in uracil. Surfaces were generated with Chem3D 5.0 software (Cambridge Soft) from the difference between the Gaussian 98 cube file corresponding to the molecular electronic density and that of the electronic density perturbed by the deletion of the selected interaction. Yellow surfaces (negative) indicate a decrease in charge density by effect of the interaction, whereas white surfaces (positive) indicate an increase in charge density. The interactions considered and the values of the isodensity surfaces shown are as follows: (a) $\pi(C_5{=}C_6) \rightarrow \pi^*(C_4{=}O)$ (*1*), ±0.0016 au; (b) $n(N_3) \rightarrow \pi^*(C_4{=}O)$ (*2*), ±0.0022 au; (c) $n_\pi(O_4) \rightarrow \sigma^*(N_3{-}C_4)$ (*6*), ±0.0016 au. (Oxygen atoms are shown in red, nitrogen atoms are blue, and carbon atoms are dark gray.)

3.2. Effect of Stereoelectronic Interactions on the Electronic Charge Density. The present formalism can be applied either to local magnitudes (e.g., atomic properties) or to delocalized or density properties (e.g., scalar or vectorial fields). The most significant scalar field at the molecular level is the electronic charge density; its analysis, in terms of deletions of selected stereoelectronic interactions, shows, in a straightforward manner, how these interactions modify the distribution of charge.

Interactions between occupied orbitals from a NBO localization do not produce a net transfer of charge, but rather redistributions within the regions occupied by each orbital, with the total charge of each orbital remaining mostly unchanged.[32] This is a consequence of the exchange antisymmetry property of the wave function, according to which a disturbance in a σ_i orbital that distorts the spatial distribution of charge requires a compensatory change in another σ_j orbital to maintain their mutual orthogonality. In contrast, delocalization interactions that involve donor−acceptor orbitals produce a net transfer of charge between them, followed by a redistribution of charge. Because delocalization interactions involve localized orbitals, their main effects are manifested locally, e.g., modulating the charge distribution near the atoms that are involved in the respective bonds. However, considering the molecule in its entirety, these interactions are also important, because they transmit the effect of different disturbances, such as changes in the molecular geometry or substituents.

The effects of stereoelectronic interactions on the charge density of uracil may be visualized with the previously outlined methodology, from the difference between the charge density calculated with and without the deletion of selected interactions. Figure 4 shows the redistribution of charge associated to representative interactions; as expected, the net charge of the difference distribution is zero. In the case of interaction *1*, $\pi(C_5{=}C_6) \rightarrow \pi^*(C_4{=}O)$ (Figure 4a), the major variations of charge density are located in regions where the density of the intervening orbitals $\pi(C_5{=}C_6)$ and $\pi^*(C_4{=}O)$ take their maximum values, in agreement with the corresponding resonance substructure (Figure 2). A decrease in charge density is observed for the donor orbital, and an increase in charge density is observed for the acceptor orbital. In addition, a redistribution of charge of opposite sign takes place in regions located between the lobes of the $\pi(C_5{=}C_6)$ orbital. This redistribution is approximately constant over the $\pi(C_5{=}C_6)$ orbital and appears as a density increase along the line joining both atoms, slightly larger over C_6. For the carbonyl at position 4, the expected decrease of charge density in the zone located between the lobes of the $\pi^*(C_4{=}O)$ antibond shows a maximum intensity over each atom (C_4 and O_4).

The effect of interaction *2*, $n(N_3) \rightarrow \pi^*(C_4{=}O)$, has features similar to those of interaction *1*, because both interactions are equivalent, resulting in a decrease in the charge density of the nonbonding pair $n(N_3)$ and an increase in the charge density in the region of the $\pi^*(C_4{=}O)$ antibond (Figure 4b). A change of opposite sign in the charge density is observed between the π lobes, especially near the positions of the N_3, C_4, and O_4 nuclei. The charge density increase over the $N_3{-}C_4$ bond arises from a cooperative effect that produces an enhancement of interaction *6*, which is a topic that is discussed below, when dealing with influences between interactions. Conversely, an anticooperative effect of interaction *2* over interaction *1* results from their sharing of the acceptor $\pi^*(C_4{=}O)$ antibond orbital; this reduces the donor capability of the $\pi(C_5{=}C_6)$ orbital and results in an increase in the charge of π-type symmetry over the $C_5{=}C_6$ bond. This increase is especially noticeable at the C_6 nucleus, in accord with the corresponding resonant substructure.

Interaction *6* decreases the charge density in the higher-probability region of $n_\pi(O_4)$ (Figure 4c). Concurrently, a strong accumulation is observed in the region of the π lobes, centered at O_4 and extending in the direction of the molecular plane. As expected from the resonant substructure corresponding to this delocalization (Figure 2), this redistribution of charge also induces a decrease of the charge density in the opposite side of the orbital, next to the C_4 atom, which results in an increase of the formal charge of C_4 (0.0353 au) and a decrease of the formal charge of O_4 (−0.0232 au).

Figure 4c also shows the cooperative effect of interaction *6* over interaction *2*. Through its acceptor orbital $\sigma^*(N_3{-}C_4)$, interaction *6* increases the charge density in the vicinity of N_3 and decreases it near C_4. The latter results from the inductive effect produced by the decrease of charge of $n_\pi(O_4)$ that also affects the $\pi^*(C_4{=}O)$ antibond. In this way, the strong localization of the nonbonding lone pair on O_4 causes the polarization of the C=O bond and the concomitant polarization of the $C_4{-}N_3$ bond. The charge density increase at N_3 results in a decrease in the density of $n(N_3)$ via interaction *2* and a transfer of charge to the $\pi^*(C_4{=}O)$ antibond. This effect, which results from the strong interrelation between interactions in cyclic compounds,[26] will be considered again when atomic charges are involved.

The aforementioned results show that, when an orbital of π symmetry is involved in a donor−acceptor interaction, the change in the charge distribution is not uniform over the entire π orbital. This change is dependent on the proximity of other orbitals that participate in the interaction and the electronegativity of the adjacent atoms. The σ orbital located between the same pair of atoms also undergoes a redistribution of charge. In the region in which the charge distributions of the σ and π orbitals are superimposed, the changes in the charge density are the same. Conversely, in other regions, where a null or a

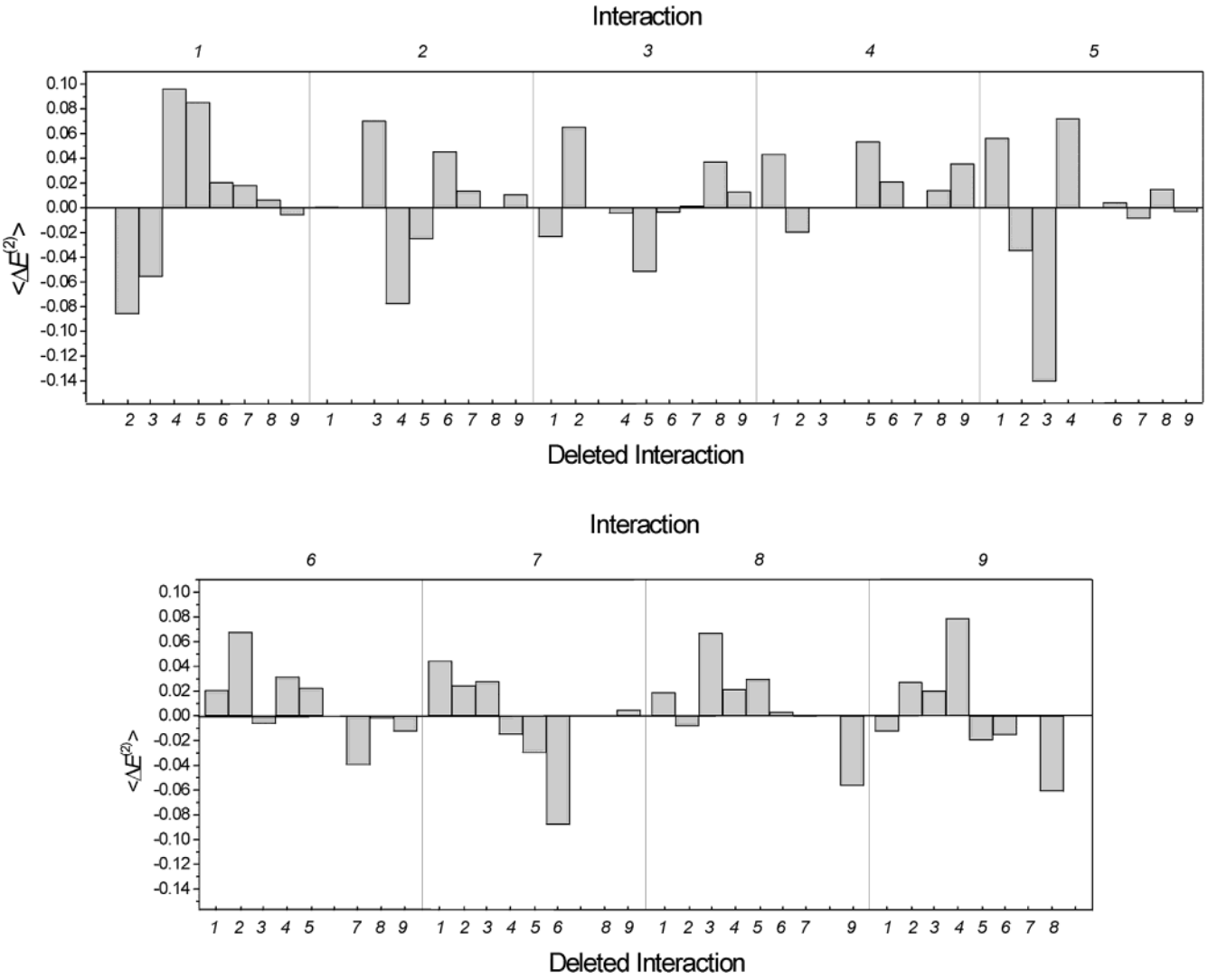

Figure 5. Influences between interactions. For each stereoelectronic interaction indicated at the top, the effects of deleting each of the remaining eight most significant interactions are depicted (see Figure 2 for notation). A positive value of the mean difference $\langle \Delta E^{(2)} \rangle = 2(E^{(2)} - E^{(2)\prime})/(E^{(2)} + E^{(2)\prime})$ implies a reinforcement of the influenced interaction (cooperativity), whereas a negative value corresponds to a reduction (anticooperativity).

small superposition takes place, an induced redistribution of charge has a tendency to compensate the change. All changes take place with negligible variations in the occupation number of the σ orbital. Overall, charge redistribution provides a means to visualize how influences between interactions take place.

3.3. Transmission of Information between Different Parts of the Molecule. Although NBO orbital diagrams have been used to rationalize cooperative effects between LMOs qualitatively,[33] a quantitative approach to the influences between interactions is not available. The general methodology depicted in Scheme 1 allows a systematic analysis of cooperative and anticooperative effects, as well as the evaluation of the net result of influences with opposite effects.

To evaluate how the deletion of each individual interaction in Figure 2 affects the remaining eight interactions in uracil, an NBO analysis was performed in each case, according to Scheme 1. As shown in Figure 5, different interactions affect a given interaction with different intensities. A clear distinction can be made between those that reinforce its value (cooperative influences) and those that diminish it (anticooperative influences). Because interactions may differ widely in the absolute value of the second-order energy lowering, a mean difference $\langle \Delta E^{(2)} \rangle = 2(E^{(2)} - E^{(2)\prime})/(E^{(2)} + E^{(2)\prime})$, where $E^{(2)\prime}$ is the value of the second-order energy lowering of a given interaction upon deletion of another interaction, was evaluated to make the influences quantitatively comparable.

A given interaction affects adjacent ones and, through them, is able to affect other interactions. The precise relationships can be deduced from the effects of deletion of interactions on the charge density or on the occupancies of other NBOs. As a working example, the effects produced by interaction *3* are considered. This interaction is a cooperative influence of interactions *8* and *9* and is anticooperative with respect to interaction *5* (Figure 5). These relationships become evident when considering the equivalent resonance substructures in Figure 2. The primary effect of interaction *3* is to decrease the occupancy of the nonbonding lone pair $n(N_1)$ and increase that of the antibonding $\pi^*(C_2{=}O)$ orbital; in addition, several indirect responses are also observed (Figure 6). A decrease in the occupancy of the $n_\pi(O_2)$ lone pair and an increase for the $\sigma^*(N_1{-}C_2)$ antibonding orbital correspond to the increase in the intensity of interaction *8*, whereas the anticooperative effect on interaction 5 is evidenced by the decrease in the occupancy of the $\pi^*(C_5{=}C_6)$ antibond orbital. The larger effect on interaction *8*, in comparison to that for interaction *9*, may be rationalized, considering that the $\sigma^*(N_1{-}C_2)$ orbital has a greater

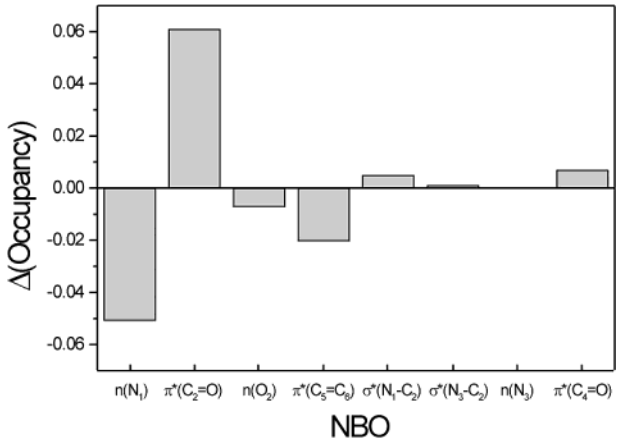

Figure 6. Effect of interaction *3* on the occupancies of selected NBOs.

tendency to attract charge density than the $\sigma^*(N_3-C_2)$ orbital, because of the density deficiency of the charge produced in the N_1-C_2 bond by the donor effect of interaction *3*.

As mentioned previously, interactions may influence each other directly or they may do it indirectly, through other interactions. A direct influence arises when an orbital that is involved in one of the interactions shares at least one atomic center with an orbital of another interaction. When this is not the case, indirect influences may take place between interactions, through a "path" of linked direct influences. Although several possible pathways may be found in each case, the more-efficient pathways should be those involving the strongest influences and the least steps (see Supporting Information for plausible two-step paths for the major indirect influences in Figure 5).

We can now gain further insight into the way in which direct influences occur. In the simplest case, for two interactions that share the same electron-donor orbital, its delocalization into the antibonding orbital of one interaction hinders the delocalization into the electron-acceptor orbital of the other interaction. The magnitude of the influence has a direct relationship with the intensity of the involved interactions; i.e., the more intense the interaction, the greater its influence over the other interaction. Pairs of interactions that show this type of anticooperative influence include interaction pairs *2*−*4*, *3*−*5*, *6*−*7*, and *8*−*9* (Figure 5).

A second class of direct influence is between an interaction involving an electron-donor orbital that shares at least one atomic center with the antibonding orbital of another interaction. Thus, the charge transferred by the latter interaction to the antibonding orbital can induce an increase in the intensity of the interaction involving the electron-donor orbital with the common atomic center and vice versa. This class of influence is cooperative and is observed for the interaction pairs *1*−*5*, *4*−*6*, *5*−*8*, and *2*−*9*.

The third class of direct influence is anticooperative and involves two interactions with antibonding orbitals that share at least one atomic center. Interaction pairs in this group include *1*−*2* and *3*−*4*, which influence each other anticooperatively, because the donor effect of one interaction is reduced by the increase in occupancy of the shared electron-acceptor orbital due to the other interaction (not fully evident in Figure 5, see below). Pairs *5*−*7* and *6*−*9* do not include the same antibond but instead include antibonds that share a common atomic center with similar results. In the case of pairs *6*−*7* and *8*−*9*, which are also of the first class, this type of influence reinforces that previously mentioned. Pairs *1*−*6*, *1*−*7*, *2*−*6*, *2*−*7*, *3*−*8*, *3*−*9*, *4*−*8*, and *4*−*9* display a combination of the second and third class of influences; in all cases, the second type prevails and net cooperative influences result.

Influences between interactions that share the same antibond orbital are not apparent from a direct analysis of Figures 4, 5, or 6, because these reflect only the final effect of the deleted interaction. This is the case of the influence that interaction *1* exerts over interaction *2*, and the mutual influences of interactions *3* and *4*. These "hard to see" effects are originated in the presence of an electron-donor orbital that delocalizes charge toward two different centers. Taking the influence of interaction *3* over interaction *4* as a working example, the direct effect of the former is the increase of occupancy of the $\pi^*(C_2{=}O)$ antibond (Figure 6). This effect induces a reduction of the intensity of interaction *4*, increasing the $n(N_3)$ occupancy; this excess of charge is efficiently delocalized into the $\pi^*(C_4{=}O)$ antibond via interaction *2*. The net result of these delocalizations is an increase of the occupancy of the $\pi^*(C_2{=}O)$ and $\pi^*(C_4{=}O)$ antibonds, because of interaction *3* in the former and interaction *2* in the latter, but a null net effect on the occupancy of the $n(N_3)$ lone pair, with interaction *4* appearing to be unchanged. A related class of anticooperativity has also been observed when analyzing H-bond networks within the quantum cluster equilibrium model, where a ternary cluster is anticooperative when a single coordination site of the central monomer is a double acceptor.[33]

The ability to delocalize charge over two electron receptor centers is dramatically illustrated when comparing the mutual influences of interactions *1* and *2*. Although the net influence of interaction *1* over interaction *2* is negligible, because of the additional delocalization of the donor orbital of interaction *2* via interaction *4*, the $\pi(C_5{=}C_6)$ bond orbital involved in interaction *1* cannot delocalize its charge over other vicinal antibonds with the same efficiency as $n(N_3)$ does. This results in a net increase of the electronic charge of the $\pi(C_5{=}C_6)$ bonding orbital with a consequent strong decrease of intensity for interaction *1* (Figures 4b and 5).

Different intensities within each group of interactions depicted in Figure 2 may be easily interpreted, in terms of the relative strength of cooperative influences of other interactions (Figure 5). Interactions that share an electron-donor lone-pair orbital may have different intensities, because their mutual anticooperative influences may differ. Thus, interaction *4* has a stronger anticooperative influence over interaction *2* than interaction *2* does over interaction *4*, making interaction *4* more intense. The same is valid for interactions *3* and *5*. Because interactions *2* and *4* share the $n(N_3)$ lone pair, and interactions *3* and *5* share the $n(N_1)$ lone pair, other interactions that influence the common donor orbital affect both members of the pair simultaneously. In the first case, interactions *6* and *9* have a direct cooperative influence on both interactions, whereas in the latter case, only interaction *8* directly influences each interaction in a cooperative sense. Interactions *6*, *9*, and *8* are equivalent interactions; therefore, the reinforced cooperativity on the first case results in interaction *4* being more intense than interaction *3*, and interaction *2* being more intense than interaction *5*. Similar conclusions may be drawn for the group of interactions that include the oxygen lone pairs, $n_\pi(O) \rightarrow \sigma^*(C-C/N)$ (interactions *6*, *7*, *8*, and *9*).

3.4. Analysis of Molecular Properties. As already mentioned, the carbonyl groups in uracil—and especially their oxygen atoms—are relevant to the biological properties of the molecule. The effect of a substituent on the properties of these carbonyls may be interpreted in terms of stereoelectronic interactions that, being strongly interconnected, play a major

TABLE 1: Effect of Selected Stereoelectronic Interactions on Carbonyl Properties of Uracil[a]

	ΔBO (au)		Δ*Q* (au)						Δσ (ppm)	
interaction	C_2═O	C_4═O	C_2	O_2	$C_2 + O_2$	C_4	O_4	$C_4 + O_4$	O_2	O_4
1	−0.0030	−0.0355	−0.0020	−0.0011	−0.0031	−0.0040	−0.0164	−0.0204	3.287	24.203
2	0.0138	−0.0415	−0.0110	0.0148	0.0038	−0.0111	−0.0172	−0.0283	−9.172	37.635
3	−0.0412	−0.0028	−0.0075	−0.0185	−0.0260	−0.0066	0.0008	−0.0058	38.615	−3.753
4	−0.0460	0.0146	−0.0110	−0.0198	−0.0308	−0.0106	0.0151	0.0045	41.061	−15.286
5	0.0164	−0.0103	−0.0100	0.0162	0.0062	0.0053	−0.0113	−0.0060	−13.058	17.887
6	−0.0054	−0.0062	−0.0005	−0.0053	−0.0058	0.0353	−0.0232	0.0121	2.712	63.536
7	−0.0014	−0.0092	0.0002	−0.0014	−0.0012	0.0244	−0.0142	0.0102	1.100	16.212
8	−0.0056	−0.0025	0.0284	−0.0165	0.0119	0.0008	−0.0028	−0.0020	22.228	3.445
9	−0.0072	−0.0043	0.0278	−0.0176	0.0102	−0.0007	−0.0042	−0.0049	21.855	2.753

[a] See Figure 1 for atom numbering and Figure 2 for interactions notation; *Q* represents atomic charge, and BO represents bond order.

role in the transmission of information from one part of the molecule to the other. An application of the present formalism follows, to study three representative properties on both carbonyl groups in uracil: bond orders (a bond property), atomic population analysis or atomic charges (an atomic property that can be added to evaluate the bond charge), and ^{17}O chemical shifts (a nonadditive local property). In addition, the effect on these properties of two representative substituents in position 5 is interpreted in the light of these results.

For practical reasons, we have defined a local Cartesian coordinate system, relative to each carbonyl group, to visualize the spatial distribution of the analyzed properties. In this Cartesian system, the ***x***-axis is normal to the plane of the carbonyl, the ***y***-axis is in the plane of the carbonyl group and is perpendicular to the C═O bond, and the ***z***-axis is aligned with the carbonyl bond.

3.4.1. Bond Orders. Several methods may be used within the NBO formalism to evaluate bond orders.[34b,35,36] Because these methods are based on the same NBO localization formalism that is used in the deletion procedure, they reduce the computational cost and make bond orders more sensitive to interactions between NBOs. Bond orders were calculated according to Wiberg's method[36] applied to the natural atomic orbital (NAO) basis (i.e., the sum of squares of off-diagonal density matrix elements between atoms, in terms of the NAO basis set). This index is routinely calculated in the NBO program as a general guide to bond order in the search for an NBO natural Lewis structure.[31]

The qualitative behavior of bond orders upon the effect of delocalizations can be rationalized in terms of resonance substructures (Figure 2). The hyperconjugative donation from a donor orbital to a vicinal antibond π^*(C═O) orbital (interactions *3* and *4*) is associated with weakening of the C═O bond and reduction of the bond order. The antibond π^*(C═O) behaves as an electron-acceptor orbital for both interactions; thus, an increase of the π^*(C═O) occupancy reinforces its antibond character, decreasing the bond order. Conversely, interactions that include the n_π(O) lone pair (interactions *8* and *9*) increase the bond order. However, as discussed when dealing with electron density, they also induce a cooperative effect on interactions *3* and *4*, which reduces the carbonyl bond order. Evaluation of these opposite effects gives a net reduction of the bond order (Table 1). Similar effects are observed in the bond order of the carbonyl in position 4. These results show that bond orders are mainly determined by the direct effect of the interactions that involve the corresponding bond or antibond orbital, in this case, π^*(C═O).

3.4.2. Atomic Charges. Atomic charges were calculated by NBO population analysis. The atomic population of each atom was calculated as the sum of the occupation numbers of all the NAOs corresponding to that atom. The atomic charge of an atom was obtained by subtracting this magnitude from the atomic number.[7] Typically, interactions between molecular orbitals (NBOs) produce transfers of charge among them, altering their occupancies. NBOs can be spanned, in terms of NAOs; therefore, the latter also undergo a change in their occupancies that is reflected in the atomic charge.

TABLE 2: Effect of Selected Stereoelectronic Interactions over Carbon and Oxygen Natural Atomic Orbitals (NAOs) of Uracil Carbonyl C_2═O[a]

	Δ(Occupancy) of Valence NAOs			
interaction	2s	$2p_x$	$2p_y$	$2p_z$
		C_2 Atom		
3	−0.0111	0.0303	−0.0125	0.0001
4	−0.0125	0.0355	−0.0130	0.0000
8	−0.0071	−0.0194	0.0082	−0.0091
9	−0.0068	−0.0187	0.0074	−0.0091
		O_2 Atom		
3	−0.0031	0.0318	−0.0072	−0.0028
4	−0.0035	0.0352	−0.0082	−0.0038
8	−0.0013	0.0280	−0.0251	0.0156
9	−0.0013	0.0275	−0.0233	0.0153

[a] See Supporting Information for data on C_4═O.

The relevant molecular orbitals that involve the carbonyl oxygen atom also affect the carbonyl carbon atom; therefore, the occupation numbers of both carbon and oxygen atoms were analyzed in terms of the deletion of interactions. Interactions that have the π^*(C═O) antibond as an acceptor orbital increase the total electronic charge of both carbonyl atoms. This is the case for interactions *1* and *2* for the C_4═O carbonyl and interactions *3* and *4* for the C_2═O carbonyl (Table 1).

As expected from the corresponding resonance substructures, the overall effect of interactions *3* and *4* on individual atomic charges is an increased polarization of the C_2═O carbonyl. The atomic charges of the carbon and oxygen atoms decrease, with a greater change on the latter. For C_2, the charge changes as the result of two opposite effects, which are the increase of the $\pi^*(C_2$═O) antibond occupancy and the decrease of the contributions of the $\sigma(N_1-C_2)$ (interaction *3*) or $\sigma(N_3-C_2)$ (interaction *4*) orbitals, the latter of which is due to the donation feature of the respective *n*(N) orbitals. Overall, the effects of relevant interactions on the other carbonyl, C_4═O, are qualitatively similar to those described previously.

The effects of these interactions on the NAO occupancies give further insight into the spatial redistribution of electronic charge around each nucleus (Table 2). The increase of electronic charge of the C_2═O carbonyl due to interactions *3* and *4* is approximately equally distributed between the p_x NAOs of the carbon and oxygen atoms, with a slightly larger value on the oxygen atom. These changes are a consequence of the $2p_x$ NAO being the main contributor to the acceptor π^*(C═O) antibond (>99% relative contribution within each of the atomic contribu-

tions to the π^*(C═O) NBO). Moreover, a decrease of occupancy is observed in the p_y and s NAOs of the carbon atom. This reduction may be related to a certain degree of delocalization toward the adjacent sigma orbitals and the induced decrease of carbon electronic charge (Table 1). In the case of interaction *2*, the delocalization is along the N_3-C_4 and C_4-C_5 bonds (Figure 4b). These orbitals are sp^2 hybridized, with a relative contribution to carbon NAOs of ca. 60% p_y and 30% s valence orbitals. Equivalent interactions (interactions *1*, *3*, and *4*) follow similar trends. On the other hand, variations of NAO oxygen occupancies in the ***z***- and ***y***-axis directions are considerably smaller than variations in the ***x***-axis direction.

The other significant interactions that involve carbonyl orbitals, interactions *6* and *7* in the case of C_4═O, and interactions *8* and *9* in the case of C_2═O, also increase the carbonyl polarization by increasing the atomic charge of the carbon atom and decreasing that of the oxygen atom. This decrease is opposite to what is expected from the resonance substructures associated with these interactions (Figure 2), because the nonbonding lone pairs of the oxygen atom are electron donors. The observed behavior arises from a combination of interactions that influence each other. Thus, interaction *8* "extracts" electronic charge from the lone pair of π symmetry of O_2 in the ***y***-axis direction, reducing the occupancy of p_y, which contributes >99% to the n_π(O) NBO and transfers part of it to the $n(N_1)$ orbital through the $\sigma^*(N_1-C_2)$ antibond, increasing the occupancy of the $\pi^*(C_2$═O) orbital (via interaction *3*). This charge undergoes a subsequent redistribution along the carbonyl bond, because of the asymmetry that is introduced by interaction *8*, which involves only one center of the carbonyl bond. This redistribution is evident from the reduction of the occupancy of the p_x and p_z valence NAOs of the carbon atom and the corresponding increase on the side of the more electronegative oxygen center (Table 2), giving back more electronic charge to the O_2 in the ***x***-axis direction (p_x) than that extracted from it in the ***y***-axis direction (p_y). Interactions *6*, *7*, and *9* follow similar mechanisms.

Overall, interactions *1*, *2*, *3*, and *4* exert their effects mainly on the entire bond of the corresponding carbonyl (compare with their effects on the bond orders). Interactions *6*, *7*, *8*, and *9* are mostly related to charge redistribution, because they involve NBOs localized over a single atom of the carbonyl group.

3.4.3. ^{17}O Chemical Shifts. ^{17}O chemical shifts were calculated using the GIAO method (Table 1).[37,38] The difference between the σ_{iso} values of O_2 and O_4 calculated with the HF/6-31+G** basis set gives 96.746 ppm, with O_2 being the most shielded nucleus. This compares reasonably well with the experimental value of 82 ppm,[39] obtained from the solution NMR spectrum of uracil in dimethylsulfoxide (DMSO), where H-bonds with the carbonyl oxygen atoms are not present. Better basis sets, such as HF/6-311+G(2d,p) (100.678 ppm) or the correlated B3LYP/D95** (97.345 ppm) that reproduces experimental trends of ^{17}O magnetic nuclear shieldings in amides very well,[40] did not improve the value obtained with the more modest basis set used in this work. Interactions *3* and *4*, which involve carbonyl acceptor orbitals, increase the O_2 shielding whereas interactions *5* and *2* decrease the shielding, through their respective anticooperative influences (Table 1). Interactions *8* and *9*, which include carbonyl donor orbitals, show a behavior similar to that of interactions *3* and *4* but with lower effects over the shielding, in accord with their relative intensities (Figure 3). In the case of O_4, the effect of interaction *2* on the shielding is more intense than that of interaction *1*, probably because the former is more efficient, in terms of delocalization energies ($E^{(2)}(2) > E^{(2)}(1)$) (Figure 3). Interaction *4* has a deshielding effect on O_4 through its direct anticooperative influence on interaction *2*. Interaction *6* has a stronger effect than interactions *1*, *2*, and *7*, probably because of the relative importance of the intensity of interaction *6* and its effect on carbonyl polarization, as explained when dealing with atomic charges.

TABLE 3: Effect of Selected Stereoelectronic Interactions on the $^{17}O_2$ Induced Shielding Tensor ($\sigma^{(i)}$) Components of Uracil[a]

	Tensor Component (ppm)			
interaction	$\Delta\sigma^{(i)}_{xx}$	$\Delta\sigma^{(i)}_{yy}$	$\Delta\sigma^{(i)}_{zz}$	$\Delta\sigma^{(i)}$
3	10.531	50.128	57.392	39.351
4	7.255	58.674	60.043	41.991
8	−13.984	24.390	46.697	19.034
9	−12.522	24.123	45.386	18.996

[a] The shielding tensor components without deletions are $\sigma^{(i)}_{xx} = -69.548$ ppm, $\sigma^{(i)}_{yy} = -460.697$ ppm, $\sigma^{(i)}_{zz} = -497.936$ ppm, and $\sigma^{(i)} = -342.727$ ppm.

A comparative analysis of atomic charges and shielding constants of the carbonyl oxygen atoms shows that the effects of all the interactions considered have approximately the same relative senses and intensities. These similarities suggest that the redistribution of charge among the orbitals adjacent to the oxygen atom due to stereoelectronic interactions is important in determining the ^{17}O shielding.

In view of these findings, a more detailed study was performed on the relationship between shieldings and orbital occupancies. The ^{17}O shielding tensor may be split into two terms; one is a shielding term (diamagnetic) that is dependent only upon properties of the electronic ground state. We will adopt the label "unperturbed" (*u*) for this term. The other is deshielding (paramagnetic) and originates in charge circulation that is associated with occupied−vacant transitions.[41] Within the NBO framework, this contribution is associated with donor−acceptor interactions.[19] Contributions arising from the excitation of the density by the magnetic field perturbation will be dubbed "induced" (*i*).[42] An individual analysis of the contributions to the GIAO shielding tensor shows that almost all the variation of the shielding due to stereoelectronic interactions comes from the induced contribution (compare Tables 1 and 3), which is in accord with general results that were stated in the early works of Ramsey[43] and Cornwell.[44] This contribution originates in electronic excitations that involve local circulating currents, which result in deshielding diagonal tensor components perpendicular to the electron motion plane.[41]

The interactions that mostly affect oxygen shieldings are those involving orbitals that include this atom center and imply a circulation of charge.[45] These interactions include both vicinal (as those analyzed in previous sections) and nonvicinal interactions. Among the latter, the most important interactions include[45] the interaction $n_\pi(O) \rightarrow \pi^*$(C═O) (magnetic vector in the *z*-axis), which corresponds to a redistribution of charge in the *xy* plane, because the n_π(O) NBO has a preponderant orientation along the ***y***-axis and the π^*(C═O) antibond along the ***x***-axis. The magnetic vector in the ***y***-axis corresponds mainly to the interaction $n_\sigma(O) \rightarrow \pi^*$(C═O), which generates local currents approximately parallel to the *xz* plane, as a consequence of n_σ(O) being preponderantly oriented along the ***z***-axis. Finally, the component in the ***x***-axis direction results from the local interaction $n_\pi(O) \rightarrow \sigma^*$(C═O), which corresponds approximately to currents in the carbonyl plane.

These magnetic-relevant geminal interactions are directly influenced by the transmission of information-relevant vicinal ones, which involves orbitals sharing at least one atomic center.

TABLE 4: Effect of Selected Stereoelectronic Interactions over Natural Bond Orbitals (NBOs) Adjacent to O_2

	Δ(Occupancy) of Valence NBOs			
interaction	n_σ(O)	N$_\pi$(O)	σ^*(C═O)	π^*(C═O)
3	−0.00086	−0.00718	−0.00061	0.06097
4	−0.00096	−0.00815	−0.00081	0.06950
8	0.00086	−0.02467	0.00003	0.00720
9	0.00090	−0.02295	0.00001	0.00750

Although delocalization energies of these geminal interactions are too small to extract conclusive results from the deletion method ($E^{(2)}$ < 0.05 kcal/mol), a way of capturing a physical manifestation of their effects is by inspection of the occupancy change of the involved NBOs, as discussed in the previous sections and in related works.[33] It should be noted that magnetic-relevant geminal interactions are much less intense than the vicinal interactions *1*−*9*, and their responses produce only minor changes in the NBO occupancies.

Table 3 shows that all the variations of these components are positive, except for those of $\sigma^{(i)}_{xx}$, because of interactions *8* and *9*. The latter, being of the n_π(O) → σ^*(C−N) type, involves charge circulation in the *yz* plane and gives a paramagnetic, negative contribution to the $\sigma^{(i)}_{xx}$ shielding component.

The intensity variations of the magnetic-relevant nonvicinal interactions produced by the influence of vicinal ones are evidenced in the occupancy changes shown in Table 4. These may be correlated with the corresponding changes in the diagonal components[46] of the induced shielding tensor. The most intense component in ^{17}O carbonyl shielding, σ_{zz}, is also the component most affected by vicinal interactions. Interactions *3* and *4* act directly over the π^*(C═O) orbital of the magnetic-relevant n_π(O) → π^*(C═O) interaction. Interactions *8* and *9* exert their influence through an indirect effect that involve interactions *3* and *4*, as evidenced by the increase of occupancy of the π^*(C═O) antibond. Consequently, the effect of the analyzed vicinal interactions over σ_{zz} is positive, and these components are primarily responsible for the also positive variation of the isotropic value of the shielding. The effects of the remaining interactions can be easily deduced following similar reasonings.

3.5. Substituent Effects on Properties of the C_2═O Carbonyl. Substituents cause a redistribution of charge in the molecule that affects properties not only in their immediate vicinity, but also in regions that are quite far from it. In the case of the uracil molecule, it is well-known that the addition of substituents in position 5 changes some properties of the oxygen in the *para* position (O_2), which is five bonds away.[47] These long-distance effects may be analyzed, considering that the mechanism involved implies the transmission of information through a network of stereoelectronic interactions.

We selected two substituents: CF_3, which has an electron-withdrawing character, and NH_2, which is an electron donor. The tendency associated with the electron delocalization may be estimated using the σ Hammett parameter corresponding to the para position to the substituent, which is almost equal in magnitude but of opposite sign for both groups.[48] Although the value of the Hammett parameter has been determined using aromatic systems,[49] the three properties analyzed in this work follow the same trend as the σ_p parameter corresponding to 5-aminouracil, uracil, and 5-trifluoromethyluracil; i.e., the values are either larger or smaller in the substituted compounds, with respect to uracil (Table 5). This suggests that the substituents exert opposite effects on the properties analyzed, with respect to the uracil values.

TABLE 5: Property Values and the Effect of Selected Interactions for the C_2═O Carbonyl upon the Addition of C-5 Substituents[a]

substituent	σ_p	BO	ΔBO[b]	Q	ΔQ[b]	σ	Δσ[c]
NH_2	−0.57	1.6286	0.1117	−0.7240	−0.0482	59.104	−77.532
H	0	1.6309	0.1110	−0.7223	−0.0479	56.478	−66.716
CF_3	0.53	1.6514	0.1070	−0.7057	−0.0463	46.866	−29.902

[a] BO, C═O bond order; Q, O_2 atomic charge; and σ, $^{17}O_2$ shielding constant. [b] Deletion of interactions *3* and *4*. [c] Deletion of interactions *2*−*5*.

TABLE 6: Effects of Interactions over O_2 in Selected 5-Substituted Uracils[a]

	Change	
property	NH_2	CF_3
BO − BO$_{uracil}$ (au)	−0.0023	0.0205
ΔBO − ΔBO$_{uracil}$[b] (au)	−0.0007	0.0040
Q − Q_{uracil} (au)	−0.0017	0.0167
ΔQ − ΔQ_{uracil}[b] (au)	−0.0003	0.0016
σ − σ_{uracil} (ppm)	2.626	−9.613
Δσ − Δσ_{uracil}[c] (ppm)	10.816	−36.814

[a] BO, C═O bond order; Q, O_2 atomic charge; and σ, $^{17}O_2$ shielding constant. [b] Deletion of interactions *3* and *4*. [c] Deletion of interactions *2*−*5*.

As shown in Table 1, the interactions that most influence the bond order of C_2═O, and the atomic charge and magnetic shielding of O_2, are interactions *3* and *4*. In addition, analysis of the mutual influences between interactions from Figure 5 suggests that interactions *5* and *2* are mainly responsible for the transmission of information to the C_2═O carbonyl in the para position, because they are the most important influences of both interactions *3* and *4*. Inspection of the resonance substructures in Figure 2 clearly shows that C-5 substituents would strongly affect interaction *5*, which increases the electronic charge at that position. Thus, electron-withdrawing groups (e.g., CF_3) will favor this interaction, whereas electron-donating groups (e.g., NH_2) will inhibit them. The effect of these substituents on interaction *2* is less evident and probably involves (at least in part) the intermediacy of interactions *1* and *7*.

Some requirements must be fulfilled to analyze the propagation of information due to electron delocalization. First, a set of interactions must be found that, at the same time, is involved in the propagation of information through the molecule and significantly influences the analyzed property. Second, if different substituents (e.g., *i* and *j*) are considered, the effect of the interactions on the properties of interest ($\Delta P_i - \Delta P_j$) must have the same sense as the variation of the property value ($P_i - P_j$). Finally, there must be a proportional relationship between the change in the effect of the interaction ($\Delta P_i/\Delta P_j$) and the change of the property (P_i/P_j) upon the addition of different substituents.

Analysis in terms of delocalization energies can give a picture of how stereoelectronic interactions transmit information through the molecule. However, because they do not give a quantitative measure of the contribution of each interaction, they do not fulfill the second and third requirements that have been stated previously. The methodology based on the effect of deletions on molecular properties gives the necessary mathematical tools to evaluate these quantitative requirements. Thus, the variation of P and ΔP upon the addition of substituents was calculated (Table 6). In the case of the C_2═O carbonyl in the para position, the set of interactions that fulfills the first requirement is that which includes interactions *3* and *4*. As shown in Table 6, the sense of variation of ΔP due to the addition of substituents is the same as that shown by the value of the properties and is,

therefore, consistent with the second requirement. Finally, the ratio of the variation of ΔP and P for uracil and the CF_3-substituted compound also fulfills the proportionality requirement; the predicted changes for uracil and 5-aminouracil are as follows (the exact values are shown in parentheses): −0.0005 au (−0.0007 au) in the case of bond orders, −0.0002 au (−0.0003 au) for occupation numbers, and −10.06 ppm (−10.82 ppm) for the isotropic shielding. In the last case, it was necessary to add interactions *2* and 5 (major influences of interactions *3* and *4*) to improve the relationship.

In summary, it is possible to interpret all these results as interactions *2* and *5* being the most important delocalizations that carry information on the changes in C-5 substituents, and interactions *3* and *4* being those responsible for transmitting this information to the para position properties.

4. Conclusions

The most important interactions that influence the values of the localized properties on uracil carbonyls analyzed in this work are the vicinal interactions that include the π^*(C═O) orbital (adjacent to the analyzed oxygen atoms) and those which involve the oxygen lone pairs. The former are particularly important in the case of bond properties (e.g., bond orders). Although geminal interactions are too small, in terms of delocalization energies, to be analyzed by the deletion procedure, the aforementioned results show that they mediate the effects of vicinal interactions on the ^{17}O magnetic shieldings of the uracyl carbonyls.

The present procedure applied to the case of a nonlocalized property, such as the electron density, was used to generate pictorial representations of the redistribution of charge in the uracil molecule, upon delocalization interactions. The combination of this representation with the analysis of orbital occupancies gives an alternative rationalization to that depicted by resonance substructures of the ways in which localized properties are altered by stereoelectronic interactions.

Overall, the methodology developed for analyzing the dependence of molecular properties with selected stereoelectronic interactions is rigorous from a formal point of view. Despite the fact that the natural bond orbital (NBO) deletion procedure does not completely cancel the interactions, it gives a quantitative measure of the relative contributions of stereoelectronic interactions to localized and nonlocalized molecular properties. The methodology is useful to interpret which interactions influence a variety of properties such as bond orders, atomic charges, and ^{17}O chemical shifts, and to find the mechanisms of the transmission of information from one position of the molecule to another, through a network of stereoelectronic interactions. This methodology also gives insight into the mechanisms by which the magnitudes of selected properties vary, as a result of the introduction of substituents, and may be applied to the study of other properties, such as, for example, changes in the molecular conformation. The high transferability of NBOs makes the conclusions drawn from a specific example easy to be generalized for application to other compounds and properties in a straightforward manner.

Acknowledgment. We thank Universidad de Buenos Aires and CONICET (Argentina) for financial support. E.M.S. thanks Universidad de Buenos Aires for a fellowship. We also thank Professor Ruben H. Contreras for helpful discussions.

Supporting Information Available: Details of the nonstandard route used in the calculations and a specific example of an input file; schematic representations for the main paths of indirect influences in uracil; and the effect of selected stereoelectronic interactions over carbon and oxygen NAOs of uracil carbonyl C_4═O (PDF). This information is available free of charge via the Internet at http://pubs.acs.org.

References and Notes

(1) Lewis, G. N. *Valence and the Structure of Atoms and Molecules*; The Chemical Catalog Co.: New York, 1923.
(2) Foster, J. M.; Boys, S. F. *Rev. Mod. Phys.* **1960**, *32*, 300.
(3) Edmiston, C.; Ruedenberg, K. *Rev. Mod. Phys.* **1963**, *34*, 457.
(4) Weinstein, H.; Pauncz, R.; Cohen, M. *Adv. At. Mol. Phys.* **1971**, *7*, 97.
(5) Foster, J. P.; Weinhold, F. *J. Am. Chem. Soc.* **1980**, *102*, 7211.
(6) Reed, A. E.; Weinhold, F. *J. Chem. Phys.* **1983**, *78*, 4066.
(7) Reed, A. E.; Weinstock, R. B.; Weinhold, F. *J. Chem. Phys.* **1985**, *83*, 735.
(8) Reed, A. E.; Weinhold, F. *J. Chem. Phys.* **1985**, *83*, 1736.
(9) Adcock, W.; Trout, N. A. *Chem. Rev.* **1999**, *99*, 1415.
(10) Kutzelnigg, W.; Fleischer, U.; Schindler, M. *NMR Basic Principles and Progress*; Springer: New York, 1991; Vol. 23 and references therein.
(11) Kutzelnigg, W. *Isr. J. Chem.* **1980**, *19*, 193.
(12) Schindler, M.; Kutzelnigg, W. *J. Chem. Phys.* **1982**, *76*, 1919.
(13) Schindler, M.; Kutzelnigg, W. *J. Am. Chem. Soc.* **1983**, *105*, 1360.
(14) Schindler, M.; Kutzelnigg, W. *Mol. Phys.* **1983**, *48*, 781.
(15) Kutzelnigg, W. In *Nuclear Magnetic Shieldings and Molecular Structure*; NATO ASI Series C; Tossel, J. A., Ed.; Kluwer: Boston, 1993; Vol. 386.
(16) Hansen, A. E.; Bouman, T. D. *J. Chem. Phys.* **1985**, *82*, 5035.
(17) Hansen, A. E.; Bouman, T. D. *J. Chem. Phys.* **1989**, *76*, 3552.
(18) Hansen A. E.; Bouman, T. D. *Nuclear Magnetic Shieldings and Molecular Structure*; NATO ASI Series C.; Tossel, J. A., Ed.; Kluwer: Boston, 1993; Vol. 386.
(19) Bohmann, J. A.; Weinhold, F.; Farrar, T. C. *J. Chem. Phys.* **1997**, *107*, 1173.
(20) Peralta, J. E.; Contreras; R. H.; Snyder, J. P. *Chem. Commun.* **2000**, 2025.
(21) Sproviero, E. M.; Burton, G. *J. Phys. Chem. A* **2002**, *106*, 7834.
(22) Wilkens, S. J.; Westler, W. M.; Markley, J. L.; Weinhold, F. *J. Am. Chem. Soc.* **2001**, *123*, 12026.
(23) Brunk, T. K.; Weinhold, F. A. *J. Am. Chem. Soc.* **1979**, *101*, 1700.
(24) Edison, A. S.; Markley, J. L.; Weinhold, F. A. *J. Biomol. NMR* **1994**, *4*, 519.
(25) Alabugin, I. V. *J. Org. Chem.* **2000**, *65*, 3910.
(26) Alabugin, I. V.; Zeiden, T. A. *J. Am. Chem. Soc.* **2002**, *124*, 3175.
(27) Jordan, K. D.; Padden-Row, M. N. *Chem. Rev.* **1992**, *92*, 395.
(28) Naleway, C. A.; Curtiss, L. A.; Miller, J. R. *J. Phys. Chem.* **1991**, *95*, 8434.
(29) Liang, C.; Newton, M. D. *J. Phys. Chem.* **1992**, *96*, 2855.
(30) Frisch, M. J.; Trucks, G. W.; Schlegel, H. B.; Scuseria, G. E.; Robb, M. A.; Cheeseman, J. R.; Zakrzewski, V. G.; Montgomery, J. A., Jr.; Stratmann, R. E.; Burant, J. C.; Dapprich, S.; Millam, J. M.; Daniels, A. D.; Kudin, K. N.; Strain, M. C.; Farkas, O.; Tomasi, J.; Barone, V.; Cossi, M.; Cammi, R.; Mennucci, B.; Pomelli, C.; Adamo, C.; Clifford, S.; Ochterski, J.; Petersson, G. A.; Ayala, P. Y.; Cui, Q.; Morokuma, K.; Malick, D. K.; Rabuck, A. D.; Raghavachari, K.; Foresman, J. B.; Cioslowski, J.; Ortiz, J. V.; Stefanov, B. B.; Liu, G.; Liashenko, A.; Piskorz, P.; Komaromi, I.; Gomperts, R.; Martin, R. L.; Fox, D. J.; Keith, T.; Al-Laham, M. A.; Peng, C. Y.; Nanayakkara, A.; Gonzalez, C.; Challacombe, M.; Gill, P. M. W.; Johnson, B. G.; Chen, W.; Wong, M. W.; Andres, J. L.; Head-Gordon, M.; Replogle, E. S.; Pople, J. A. *Gaussian 98*, revision A.7; Gaussian, Inc.: Pittsburgh, PA, 1998.
(31) Glendening, E. D.; Reed, A. E.; Carpenter, J. E.; Weinhold, F. *NBO*, version 3.1.
(32) Reed, A. E.; Curtiss, L. A.; Weinhold, F. A. *Chem. Rev.* **1988**, *88*, 899.
(33) Weinhold, F. *THEOCHEM* **1997**, *398*, 181.
(34) (a) Glendening, E. D.; Weinhold, F. *J. Comput. Chem.* **1998**, *19*, 593. (b) Glendening, E. D.; Weinhold, F. *J. Comput. Chem.* **1998**, *19*, 610. (c) Glendening, E. D.; Badenshoop, J. K.; Weinhold, F. *J. Comput. Chem.* **1998**, *19*, 628.
(35) (a) Reed, A. E.; Schleyer, P. v. R. *Inorg. Chem.* **1988**, *27*, 3969. (b) Reed, A. E.; Schleyer, P. v. R. *J. Am. Chem. Soc.* **1990**, *112*, 1434.
(36) Wiberg, K.; *Tetrahedron* **1968**, *24*, 1083.
(37) Ditchfield, R. *Mol. Phys.* **1974**, *27*, 789.
(38) Wolinski, K.; Hinton, J. F.; Pulay, P. *J. Am. Chem. Soc.* **1990**, *112*, 8251.
(39) Wu, G.; Dong, S. *J. Am. Chem. Soc.* **2001**, *123*, 9119.
(40) Yamada, K.; Dong, S.; Wu, G. *J. Am. Chem. Soc.* **2000**, *122*, 11602.
(41) Grutzner, J. B. In *Recent Advances in Organic NMR Spectroscopy*; Lambert, J. B., Rittner, R., Eds.; Norell Press: Landisville, NJ, 1987; pp 17−42.

(42) The use of this nomenclature within the GIAO framework is in accord with that used in related works (see, for example, ref 19). In the Gaussian 98 output files, the shielding contributions are dubbed "diamagnetic" and "paramagnetic", instead of "unperturbed" and "induced".

(43) (a) Ramsey, N. F. *Phys. Rev.* **1950**, *78*, 699. (b) Ramsey, N. F. *Phys. Rev.* **1952**, *86*, 243.

(44) Cornwell, C. D. *J. Chem. Phys.* **1966**, *44*, 874.

(45) Dahn, H.; Carrupt, P. A. *Magn. Reson. Chem.* **1997**, *35*, 577.

(46) Because of the negligible effect of principal axis rotation (differences of diagonal components between Cartesian and principal frameworks are on the order of or less than 0.5%), the effects of interactions may be analyzed relating the diagonal components of the Cartesian axis system and NBOs occupancies before and after deletions.

(47) Bednarek, E.; Dobrowolski, J. C.; Dobrosz-Teperek, K.; Sitkowski, J.; Kozerski, L.; Lewandowski, W.; Mazurek, A. P. *J. Mol. Struct.* **1999**, *483*, 333.

(48) March, J. *Advanced Organic Chemistry*; John Wiley and Sons: New York, 1992; p 280.

(49) Chapman, N. B.; Shorter, J. *Correlation Analysis in Chemistry: Recent Advances*; Plenum: New York, 1978; pp 439−540.